Phonon thermal transport in noncrystalline materials*

M. P. Zaitlin[†] and A. C. Anderson

Department of Physics and Materials Research Laboratory, University of Illinois, Urbana, Illinois 61801

(Received 28 April 1975)

The thermal conductivities of a borosilicate glass and a polycarbonate have been measured in the temperature range 0.04–60 K. Some samples contained well-defined holes to provide an additional source of phonon scattering. The results at low temperatures are consistent with the predictions of the Debye model using experimentally measured sound velocities. There is a sharp decrease in phonon mean free path with increasing frequency so that, at higher temperatures (the "plateau" region), thermal transport is provided predominantly by phonons having frequencies much less that $\omega \simeq 4kT/\hbar$. For very small hole diameters, diffraction of thermal phonons occurs. The data are compared with theoretical models of thermal transport in noncrystalline materials.

I. INTRODUCTION

The thermal conductivity κ of a noncrystalline material decreases monotonically with decreasing temperature below room temperature,[1] becomes nearly temperature independent[2] near 10 K, a regime often referred to as a plateau, and below ≈ 1 K attains a temperature dependence[3,4] close to T^2. In addition, the qualitative magnitude of κ at a given temperature depends very little on the chemical structure of the material.[4] The similar magnitude and temperature dependence for all noncrystalline materials suggests that κ is independent of the details of the atomic arrangement and depends only on the fact that the structure is amorphous.

Many theoretical models have been proposed to account for this behavior of κ.[5-11] Some of these theories also attempt to explain other unusual low-temperature properties observed in amorphous systems, such as an anomalous specific heat,[4] acoustic attenuation,[12] acoustic dispersion,[13] and thermal expansion.[14] We will return to a discussion of a few of these models in Sec. IV.

Empirically it has been known from ultrasonic[12] and light-scattering[15-17] experiments that phonons propagate in noncrystalline materials at frequencies up to $\approx 4 \times 10^{10}$ Hz and thus contribute to thermal transport. Thermal phonons in this frequency range correspond to temperatures $\lesssim 0.4$ K. There is also experimental evidence of additional low-frequency (low-temperature) excitations in glassy materials.[18-21] It was the purpose of the present work to determine the relative roles of the two kinds of excitations in the thermal conductivity of noncrystalline materials.[22]

The plan was to produce phonon scattering from the surfaces of the sample. Knowing the mean free path of the phonons due to boundary scattering, one obtains from κ information on the specific heat of the phonons as well as on the phonon mean free path in the bulk material. Attempts to produce boundary scattering in thin films or plates essentially failed, as discussed in the following paper.[23] We therefore have used another method of creating phonon scattering, namely, the introduction of a large number of holes. We were able to find two very different commerical materials, a glass and a polycarbonate, which contained well-defined holes. The phonon mean free paths due to the presence of the holes could be determined from visual measurements of the sizes and densities of holes. The results of the thermal-conductivity measurements on these samples are presented in Sec. III. A qualitative explanation and analysis of the data is also given in Sec. III, and a comparison with several theories is presented in Sec. IV. In brief, our results are consistent with the heat carriers being phonons with a density of states given by the Debye model using measured acoustic velocities, and with the mean free path of the phonons decreasing rapidly with increasing frequency near 10^{11} Hz so that the thermal conductance in the plateau region is provided primarily by low-frequency phonons. With very small hole diameters diffraction of the thermal phonons becomes important. This last effect is discussed separately in Appendix A.

II. EXPERIMENT

The measurements were made on 250-μm-thick, fused capillary arrays of borosilicate glass[24] and on 6–13-μm-thick polycarbonate sheets.[25] Both materials contained well-defined cylindrical holes of uniform size oriented perpendicular to the plane of the sheets. (See the inserts in Figs. 2 and 3.) The two materials were complementary in that the glass was better characterized than the polycarbonate, but the polycarbonate had a more appropriate range of hole diameters and densities.

For the polycarbonate the hole diameters ranged from 0.03 to 8 μm and had porosities r (ratio of open area divided by total area) of 0.004–0.14,

as verified by photographs obtained from both optical and electron microscopes. The geometrical mean free path l is given by

$$l^{-1} = n \int_{-\pi}^{\pi} \sigma(\theta)(1 - \cos\theta)\,d\theta ,$$

where n is the density of holes and $\sigma(\theta)$ is the differential cross width.[26] Assuming phonon wavelengths much less than the diameter d of the holes and specular reflection of phonons at these surfaces,[23] $l = 3/4nd = 0.59d/r$.

The glass samples had hole diameters as small as 2 μm with a typical porosity of $r \approx 0.6$. The holes were arranged in a honeycomb structure, with the large-diameter holes having a hexagonal shape which became closer to circular for samples with smaller-diameter holes (see insert in Fig. 3). For this geometry, in the limit of large porosity and with specular reflection[23] from the surfaces of the pores, one would expect the mean free path to be somewhat larger than the side of a hexagon. We estimate $l \approx 1.1(\frac{3}{2}r^{-1/2} - 1)d$. This expression gives within 10% the same value as $l = 0.59d/r$ in the range of interest, namely, $0.5 < r < 0.8$, which suggests that even for large porosities $l = 0.59d/r$ applied reasonably well. The porosity was determined by weighing dry samples and utilizing the known sample volume and bulk density, and n was obtained from measurements in an optical microscope. The results are summarized in Table I.

Because of the large temperature range required (0.04–60 K), data on each sample were obtained in separate runs made either above or below ≈ 2 K. Below 2 K the most important design consideration was the very small thermal conductance of the samples. The sample length had to be kept short to minimize the effects of heat leaks and thermal time constants. A two-heater tech-
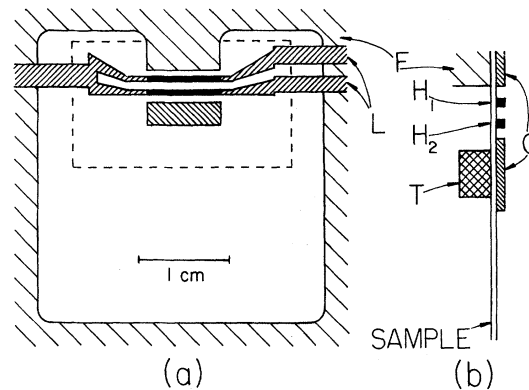

FIG. 1. Front (a) and side (b) views of sample mount. Some dimensions are exaggerated for clarity. F, thermal sink; H_1, H_2, electrical heaters; T, carbon resistance thermometer; L, superconducting leads to heaters; G, gold "isotherms." Dashed line represents the size and position of the glass samples.

nique was used, as shown in Fig. 1, rather than the more common technique utilizing two thermometers, since we could make electrical heaters narrower than resistance thermometers. To obtain a datum, power was first applied to heater H_1 and the temperature measured with thermometer T. The power was then removed from H_1 and the same power applied to heater H_2. The second reading of the thermometer T provided a temperature difference from which the thermal conductivity κ could be calculated. Throughout the measurement the thermal sink F was maintained at a constant temperature.

By using two heaters the active length of the samples could be as small as 600 μm for the low-temperature measurements. Even at this separation the heater power used at the lowest temperatures was only $\approx 10^{-11}$ W or ≈ 10 erg/day. The heaters were vapor-deposited Constantan or several hundred Å thickness, width 3×10^{-2} cm, length 0.7 cm, and resistance of ≈ 100 Ω. Only heaters having the correct measured resistivity were used to ensure a uniform film thickness and thus the absence of localized hot spots when used as a heater. Electrical leads were ≈ 4000-Å films of vapor-deposited PbSn. These films were superconducting and served to thermally isolate the active portion of the sample.

The thermometer was a chip from a Speer carbon resistor with vapor-deposited PbSn leads as discussed elsewhere.[27] This was calibrated in each run against cerium-magnesium-nitrate magnetic thermometer,[28] which in turn was calibrated against ^{3}He vapor pressure as well as several superconducting fixed points. At the lowest temperatures the power dissipated in the thermometer was limited to $\approx 10^{-14}$ W to prevent heating the thermometer above the temperature

TABLE I. Details concerning the thermal-conductivity samples. d, hole diameter; n, density of holes; r, porosity; l_h, mean free path due to holes; t, thickness; G, glass; P, polycarbonate. All values were measured except for sample $P6$, where estimates of d and n were provided by the vendor.

Sample	d (10^{-4} cm)	n (10^6 cm^{-2})	r	l_h (10^{-4} cm)	t (10^{-3} cm)
$G1$	0	0	0	$\cdots$	28.0
$G2$	53.3	0.0273	0.609	51.6	24.7
$G3$	21.9	0.157	0.590	21.8	26.5
$G4$	5.35	2.71	0.609	5.18	25.6
$G5$	2.11	16.2	0.565	2.20	23.7
$P1$	0	0	0	$\cdots$	1.32
$P2$	8.0	0.098	0.049	96	0.69
$P3$	0.80	28	0.141	3.4	1.14
$P4$	0.20	250	0.079	1.5	1.16
$P5$	0.20	100	0.031	3.8	0.96
$P6$	0.030	600	0.0042	4.2	0.60

of its environment.

The samples were mechanically and thermally anchored to the copper holder with GE 7031 varnish or epoxy as shown in Fig. 1. The polycarbonate covered the entire open area, while the glass plates were self-supporting and thus attached only to the copper finger. In the latter case, electrical connection was made to the heater leads at the edges of the glass sample by means of In wire.

At high temperatures, above 2 K, superconducting leads could not be used for thermal isolation, so fine manganin wires were used. Also the thermal time constants became long ($\gtrsim 1$ h for some samples), and so calibrated Ge resistance thermometers were used to avoid the drift associated with carbon thermometers.[29] For the glass samples, manganin-wire heaters were glued to thin Cu strips which in turn were glued to the sample. The heater separation in this case was increased to 0.2–1 cm to provide a greater accuracy in the measured length of the sample, and the heaters were extended the full width of the samples, thus providing a more simple geometry.

For the polycarbonate samples above 2 K, a holder similar to that of Fig. 1 was used for mechanical support, except that a completely circular geometry helped to minimize the thermal impedance of the sample and hence the time constant. Aluminum rings 10^4 Å thick were vapor deposited beneath the manganin-wire heaters to provide isotherms. A circular Al disk was also deposited beneath the thermometer. The electrical resistances of the Al films were checked, using the Wiedemann–Franz law, to be certain they would remain isothermal.

Before measurements were made above 2 K, the samples were "baked" in vacuum for almost a day at a temperature of ≈ 25 K. Otherwise, during measurements the sample temperature would not vary exponentially with time when a heater was energized, suggesting that a time-dependent heat leak was present. These effects were most pronounced near 9 K, and were assumed to be related to the presence of residual He (thermal exchange gas) on the sample surfaces. (Below 2 K no influence of residual He could be detected after the apparatus was baked for a period of 1 h.) For measurements above 2 K the sample holders were connected through a poor thermal link to a pumped ^{4}He stage rather than to the dilution-refrigeration stage of the cryostat. As a check, a second, less quantitative measurement of κ was obtained for the region between H_1 and F in Fig. 1 by noting the change in T before and after power was applied to H_1.

Several nonstandard computations must be applied to the measured thermal conductance to extract κ. First it is necessary to take into account the fact that some of the material has been removed from the samples to create the holes. As discussed in Appendix B, this factor is particularly important for the glass since the porosity is large, $r \approx 0.6$. If this computation were properly performed, the measured κ near room temperature, where scattering from holes cannot be important,[1] would be the same for all glass or all polycarbonate samples with or without holes.

For samples used below 2 K there are "edge effects" since the heaters do not extend the full width of the sample. The situation is analogous to the fringing electric fields of a parallel-plate capacitor. Rather than attempt to calculate the effect, the sample geometry was simulated on electrically conducting paper using the same technique as described in Appendix B. This also had the advantage that the effect of the small thermal conductance to the "sides" of the sample could be estimated at the same time. The net effect was about a 35% change in the geometrical ratio $L_2 / t L_1$, where t is the sample thickness, L_1 the heater length, and L_2 the separation *between* heaters.

Another complication occurred for the low-temperature measurements on the polycarbonate samples because of their very small thermal conductance. Some of the heat passed through the metallic heater since the thermal impedance of the heater, the polycarbonate, and the thermal boundary resistance between the two were all of the same order of magnitude. The effective length of L_2 is therefore increased by $\approx 25\%$ for $L_2 \approx 600$ μm. This was verified experimentally by changing L_2 between 200 and 1200 μm on the same material. The corrected measurements agreed to within 10%.

The geometries of samples used above 2 K were much better known, and so κ measured above 2 K could be used as a check of the calculations applied to measurements below 2 K. For both the glass and the polycarbonate the low-temperature κ data were too large by $\approx 8\%$ for every sample. Thus to provide a smooth transition between the low- and high-temperature data, those obtained below 2 K were multiplied by factors of about 0.92. Because of the several computations, the thermal-conductivity data for a given sample are considered accurate only to within a multiplicative factor which may differ from unity by $\approx \pm 10\%$.

III. DATA AND INTERPRETATION

The data for the borosilicate glass are shown in Fig. 2. For the bulk (nonporous) samples these data are in good agreement with other measurements on borosilicate glasses.[30-32] For the porous samples the presence of the holes depresses the thermal conductivity at all temperatures up to ≈ 50 K, the high-temperature end of the plateau region. The fact that the data for the porous glass
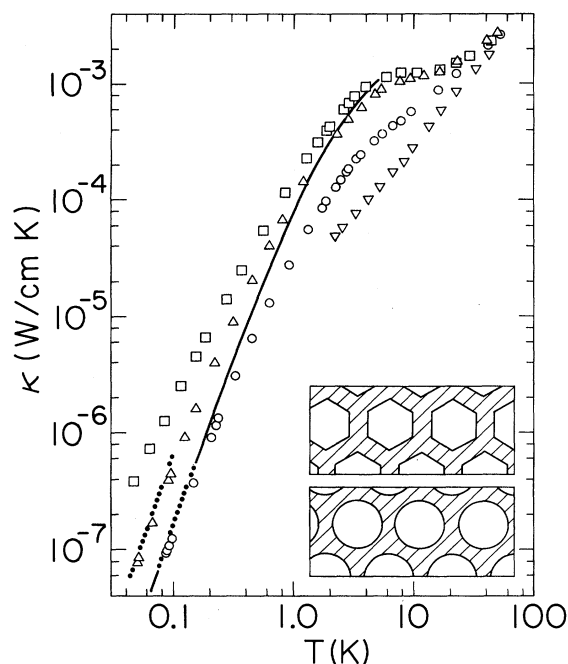
FIG. 2. Data for borosilicate glass samples. □, sample G1 (see Table I); △, sample G3; ○, sample G4; ▽, sample G5. Solid curve is a "dominant phonon approximation" for sample G4 as discussed in the text. Dotted lines were calculated, using no adjustable parameters, assuming thermal transport by phonons which have a Debye density of states and which are scattered only by the holes in the sample. Inserts show the arrangement of the holes for sample G3 (top) and samples G4 and G5 (bottom).

and the bulk glass coincide above ≈ 50 K indicates that the missing-volume calculation of Appendix B was properly performed.

The data for the polycarbonate material are shown in Fig. 3. For the nonporous samples κ is the same whether the material is unirradiated,[25] irradiated but not etched, or etched and irradiated but with a very small density of holes (sample P2), and κ is also independent of the thickness of the sheet. The data below ≈ 1 K agree in temperature dependence, and, within a factor of ≈ 2, in magnitude with measurements on materials such as Mylar,[33] polymethyl methacrylate,[34] polystyrene,[34] polycarbonate,[35] epoxy,[31] and GE 7031 varnish.[20] In brief the behavior of our low-temperature data is representative of a variety of polymer and similar materials.

Above 1 K the plateau is less pronounced than in other measurements on polycarbonate.[35] This is indicative of the presence of some crystallinity.[36,37] Indeed, according to the manufacturer,[25] the starting material for our samples was 7–9% crystalline. It is possible that the higher thermal conductivity

of the crystals thermally shunts the amorphous material at high temperatures ($T \gtrsim 3$ K), but that at lower temperatures the scattering at the amorphous-crystalline interfaces reduces κ. The net effect is to remove the plateau, as has been observed in noncrystalline materials with high-conductivity fillers intentionally added.[3,38,39] In brief, although thermal transport in the polycarbonate may be more complicated than in the glass, the polycarbonate nevertheless is representative of a broad class of materials.

The presence of the holes in the polycarbonate depressed κ just as in the glass, and in addition, the data converge at temperatures above 10 K. Also shown in Fig. 3 are data for two samples (P3, P5) having greatly different hole diameters and densities, yet nearly the same geometrical mean free path due to holes (see Table I). The thermal conductivities of the two samples are nearly the same, indicating that the reduction in κ is indeed related to the mean free path produced by the holes.

Although the two materials, glass and polycarbonate, are microscopically and chemically quite different, the thermal conductivities of both materials are influenced in the same way by the scat-
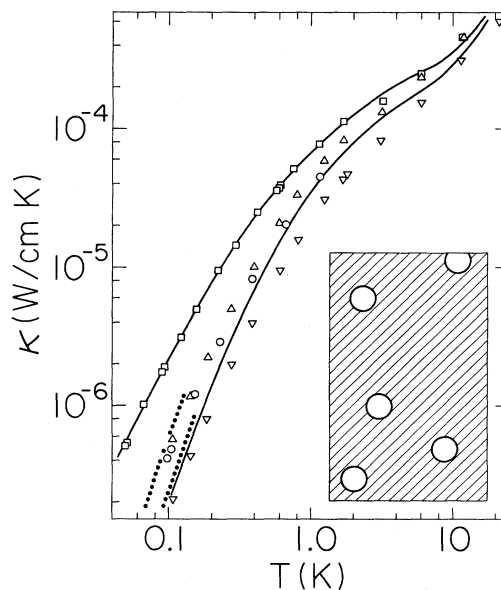

FIG. 3. Data for polycarbonate samples. □, sample P1; ○, sample P3; △, sample P5; ▽, sample P4. Insert depicts the random arrangement of the holes. Solid curves are theoretical fits of the tunneling model to P1 and P4, the latter data probably being systematically $\approx 10\%$ low as discussed in the text. Dotted lines were calculated, using no adjustable parameters, assuming thermal transport by phonons which have a Debye density of states and which are scattered only by the holes in the sample.

tering of thermal carriers from the holes. We therefore have reason to believe that conclusions based on the above data will be representative of most if not all noncrystalline materials.

We begin an interpretation of the data with a discussion of the lowest temperature measurements. As mentioned in Sec. I, phonons are known to propagate below ≈ 0.4 K. Also the κ of the porous samples has a nearly T^3 temperature dependence at the lowest temperatures. These facts suggest the use of the Debye model, giving

$$\kappa = \tfrac{1}{3}Cvl = 2\pi^2 k^4 T^3 l_h/15\hbar^3\bar{v}^2 . \qquad (1)$$

Here l_h is the mean free path due to holes (Table I), and $\bar{v}$ is an appropriate average[40] of the measured acoustic velocities.[35,41] This formula, which contains no adjustable parameters, is represented by the dotted lines in Figs. 2 and 3. The agreement between the data and this simple model is very good. This simple calculation neglects the small influence of the "bulk" scattering which is still present in the porous material. The bulk scattering may be included by using

$$\kappa_c = (\kappa_b^{-1} + \kappa_h^{-1})^{-1} , \qquad (2)$$

where κ_b is the measured thermal conductivity of the nonporous material and κ_h is the value given by

FIG. 5. (a) Qualitative frequency dependence of the phonon mean free path $l(\omega)$ in noncrystalline materials $(A\text{-}B\text{-}C)$, and the contribution $C(\omega)$ to the phonon specific heat of phonons having frequency ω as evaluated at three different temperatures (D,E,F). Line I represents the mean free path related to the presence of holes. (b) Temperature dependence of the thermal conductivity associated with the mean free paths shown in (a).
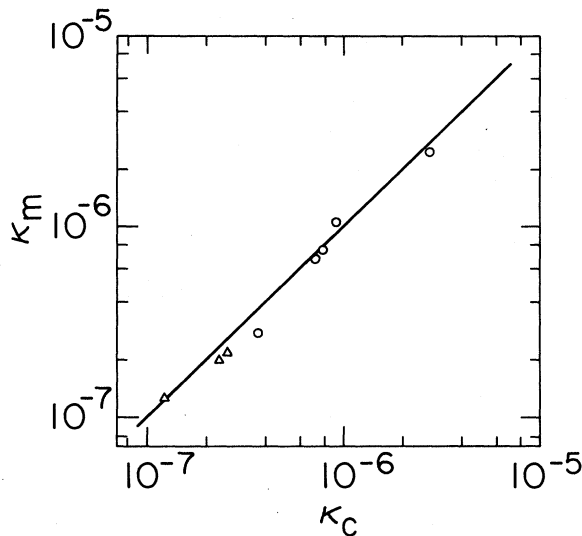

FIG. 4. Comparison of the measured thermal conductivity κ_m in the porous samples vs that κ_c, calculated from the Debye model using no adjustable parameters. Units are W/cm K. Comparison is made at 0.12 K except for two glass samples measured to lower temperatures and thus compared to 0.06 K. $\triangle$, glass samples; $\circ$, polycarbonate samples. Perfect agreement is represented by the line; the average deviation about this line is $\approx 10\%$. Alternatively this plot may be viewed as a comparison of the measured and calculated phonon mean free paths.
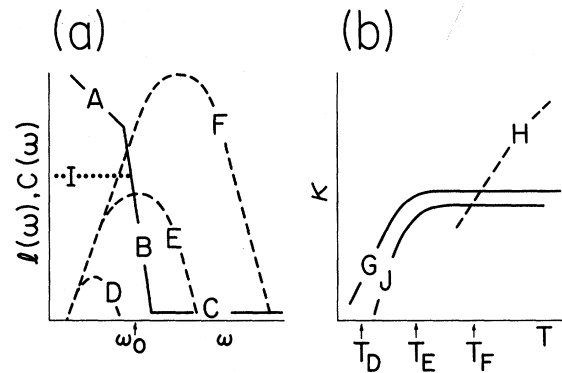
Eq. (1). This is simply Matthiesen's rule applied to phonons. This calculation is compared with the low-temperature data in Fig. 4 for all samples.

The good agreement at low temperatures between the data and the simple Debye model indicates that the thermal carriers are phonons having acoustic velocities and a Debye density of states. Thus any additional or anomalous specific heat beyond that calculated from the Debye model is to be associated with nonpropagating thermal excitations. These same conclusions concerning data near ≈ 0.1 K have been obtained by Pohl et al. for glass by measuring κ of a sample consisting of fine fibers roughened on the surfaces so as to produce boundary scattering of phonons.[42] Since these conclusions are valid for both glass and polycarbonate, they are probably true for most, if not all, noncrystalline materials.

The reduction in κ due to the holes at temperatures as high as ≈ 20 K requires a frequency-dependent phonon mean free path. This result cannot be explained by the "dominant phonon approximation" $(\omega/2\pi \approx 10^{11}T\ \mathrm{Hz\,K^{-1}})$, that is, by a purely temperature-dependent mean free path. The failure of this approach is demonstrated by the solid curve in Fig. 2, which was calculated for sample $G4$ as discussed above [Eq. (2)]. The curve clearly does not describe the behavior of the data at higher temperatures; in particular, κ in the plateau region is not depressed.

A qualitative explanation of the data is provided in Fig. 5. Both Figs. 5(a) and 5(b) are meant to represent ln-ln graphs. In Fig. 5(a) line A represents a phonon mean free path $l(\omega)$ which has a frequency dependence of ω^{-1} to account for

the essentially T^2 temperature dependence of κ at low temperatures. Line B represents an abrupt and large decrease in $l(\omega)$ near ω_0 which may be present for various reasons as discussed in Sec. IV. Line C is the minimum conceivable phonon mean free path, a few Å in length, as discussed by Kittel,[1] and as is often used to explain high-temperature data.[43] The contribution $C(\omega)$ to the phonon specific heat for phonons having frequency ω [see Eq. (5)] is also shown in Fig. 5(a) for three temperatures, namely, a low temperature T_D (curve D), an intermediate temperature T_E (curve E), and a high temperature T_F (curve F). The thermal conductivity is proportional to an integral, over frequency, of the product $C(\omega)l(\omega)$. It is instructive to divide this integral into two parts, one for low-frequency phonons having long mean free paths and the other for $\omega > \omega_0$:

$$\kappa \propto \int_0^{\omega_D} C(\omega)l(\omega)\,d\omega$$

$$= \int_0^{\omega_0} C(\omega)l(\omega)\,d\omega + \int_0^{\omega_D} C(\omega)l(\omega)\,d\omega . \quad (3)$$

Here ω_D is the Debye frequency. The first term in Eq. (3) gives curve G in Fig. 5(b). The thermal conductivity becomes constant above T_E because $C(\omega)$ at $\omega < \omega_0$ has become a constant independent of temperature. It is equivalent to having a material with a Debye frequency of ω_0. In either case there is a cutoff in the contributing modes. The second term in Eq. (3) produces curve H in Fig. 5(b). A curve of the total thermal conductivity, G plus H, therefore would contain a plateau near T_E.

To check the above ideas one introduces holes in the sample. This produces a frequency-independent l shown by line I of Fig. 5(a), and values of l larger than I (i.e., line A) are no longer of importance. The first term in Eq. (3) now gives curve J of Fig. 5(b). At low temperatures the temperature dependence of κ has changed from T^2 to T^3, and κ is depressed at temperatures up to the line H, where high-frequency phonons become important.

In brief, our data suggest that phonons conduct thermal energy throughout the temperature range of the experiments, and that the plateau region is caused by an abrupt decrease in l with increasing phonon frequency. Our data continue to be compatible with Kittel's suggested approximation of a limiting mean free path of a few Å for very-high-frequency phonons.

IV. COMPARISON WITH THEORETICAL MODELS

Many models have been suggested to explain the behavior of κ in glassy materials. Even though the discussion in Sec. III is intended to be qualita-

tive, it nevertheless can be used to determine that some models are incorrect. For example, a widely quoted suggestion by Klemens[44] that the plateau arises from the long mean free paths of longitudinal phonons at low temperatures is not consistent with our data. On the other hand we cannot rule out the possibility of a strong resonant scattering between phonons and localized excitations[45,46] which could lead to an abrupt decrease in l as indicated in Fig. 5(a). Alternatively, the decrease in l may be associated with a short correlation length in the amorphous material.[4,10,11,45] Indeed phonons in any nonhomogeneous material will have $l \propto \omega^{-4}$ (Rayleigh scattering) if the phonon wavelength λ is large relative to the size of the local fluctuations in composition.[47]

In the following we compare the data quantitatively with two models, the density-fluctuation model of Walton,[11] and the tunneling-states model of Phillips[48] and of Anderson et al.[49] Walton's model has the advantage of being mathematically very simple. In Fig. 5(a) lines B and C would in this model be related to Rayleigh and Kittel scattering as discussed above. According to Walton, line A would also be due to density fluctuations, although we do not defend this last statement. This model makes no attempt to explain the other anomalous properties of glassy materials discussed in Sec. I. The tunneling model, on the other hand, can account for a variety of properties, but is mathematically more complicated. The tunneling model as published concerns only the region A of Fig. 5(a). For B and C we will first use Rayleigh and Kittel scattering as for Walton's model. An alternative possibility will be discussed below. Neither model attempts to obtain the theoretical parameters from microscopic arguments.

The thermal conductivity is calculated from

$$\kappa = \frac{1}{3} \int_0^{\omega_D} C(\omega)\,\overline{v}l\,d\omega , \quad (4)$$

where, from the Debye model,

$$C(\omega) = 3\hbar^2 \omega^4 e^{\hbar\omega/kT}/2\pi^2 \overline{v}^3 kT^2 (e^{\hbar\omega/kT} - 1)^2 \quad (5)$$

and

$$l = (l_A^{-1} + l_B^{-1} + l_h^{-1})^{-1} \quad (6)$$

for $l > l_C$, otherwise

$$l = l_C . \quad (7)$$

The subscripts A, B, and C refer to the phonon scattering processes depicted in Fig. 5(a). For Walton's model, $l_A = A(\hbar\omega/k)^{-1}$ and $l_B = B(\hbar\omega/k)^{-4}$. In the tunneling model, $l_B = B(\hbar\omega/k)^{-4}$ again and

$$l_A = \{[(Ak/\hbar\omega)\coth(\hbar\omega/2kT)]^{-1}$$

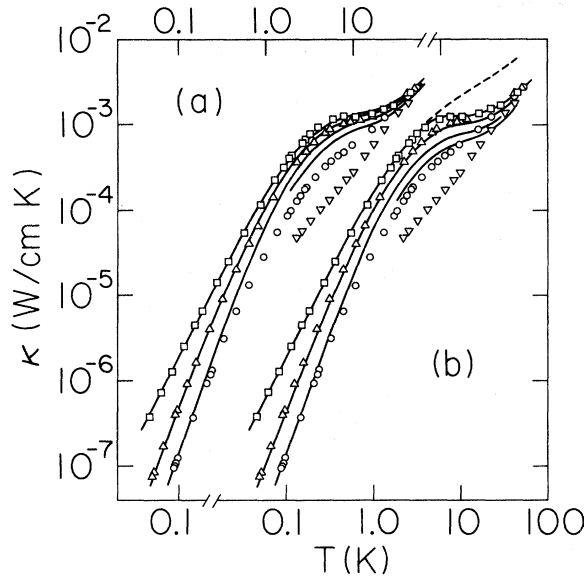$$+ (4A/\beta T^3)^{-1}\}^{-1} \text{ for } \hbar\omega/k > \beta T^3 \quad (8)$$

FIG. 6. Theoretical fits of the density-fluctuation model (a) and the tunneling model (b) to the borosilicate glass data. Symbols are the same as Fig. 2. Broken curve in (b) shows the results of omitting the nonresonant scattering of phonons.

or

$$l_A = \{ [(Ak/\hbar\omega)\coth(\hbar\omega/2kT)]^{-1}$$

$$+ (4Ak/\hbar\omega)^{-1} \}^{-1} \quad \text{for } \hbar\omega/k < \beta T^3 . \qquad (9)$$

The second term in Eqs. (8) and (9) takes into account the "nonresonant" scattering from the tunneling states as discussed by Jäckle.[50]

A comparison of these two models with the data for the glass samples is provided in Fig. 6. The Walton model provides a good fit to the data of the nonporous sample with $A = 2.11 \times 10^{-3}$ cm K, $B = 0.88$ cm K^4, and $l_C = 4 \times 10^{-8}$ cm. The frequency dependence of l_B could be increased without essentially changing the fit; with $l_B \propto \omega^{-\infty}$ (i.e., an abrupt decrease in l) the calculated plateau region is slightly more horizontal. On the other hand, $l_B \propto \omega^{-3}$ does not fit the data.

The calculations for the nonporous glass sample using the tunneling model require $A = 1.56 \times 10^{-3}$ cm K, $B = 0.47$ cm K^4, $l_C = 4 \times 10^{-8}$ cm, and $\beta = 1.5 \times 10^{-3}$ K^{-2}. This value of β is close to the value expected[50] from ultrasonic measurements on borosilicate glass.[12] The nonresonant term is essential because without it there is no mechanism to scatter low-frequency phonons at high temperature. Omitting this term gives the dashed curve of Fig. 6. It might also be noted that the presence of this term can produce a slight minimum in κ in the plateau region,[5] although this behavior is usually not observed experimentally.

It may be concluded from the foregoing that the

temperature at which the plateau is located is very insensitive to the properties of the material. Using Walton's model for convenience, the plateau "begins" because of the intersection of lines A and B of Fig. 5(a), or at a temperature of $T_p \approx (B/A)^{1/3}$. Large changes of B and/or A have little effect on T_p since line B is so nearly vertical.

The value $A = 1.56 \times 10^{-3}$ cm K obtained with the tunneling model may be compared with a value of 2×10^{-3} cm K from acoustic attenuation measurements on borosilicate glass[12] using longitudinal phonons. The implication of the agreement is that longitudinal and transverse phonons have a similar *mean free path* in bulk noncrystalline materials, as is also deduced from acoustic dispersion measurements.[13]

The value of B obtained with either model can be compared with theoretical estimates of Rayleigh scattering. Zeller and Pohl[4] have suggested an "isotopic scattering" model in which the glass is represented as a crystal with every atom displaced, and the associated vacancies provide the scattering sources. The mean free path is then[26,44]

$$l(\omega) = 4\pi v^4 [FV_0 \omega^4 (\delta\rho/\rho)^2]^{-1}$$

$$\simeq 4\pi v^4/V_0 \omega^4 , \qquad (10)$$

where V_0 is the size of the scattering center, F is the fraction of volume taken up by the scattering centers, and $\delta\rho/\rho$ is the fractional change in density within a center. Using for V_0 the value suggested by Zeller and Pohl (about the size of an atom), Eq. (10) leads to $B \simeq 20$ cm K^4, or a mean free path more than an order of magnitude *larger* than found experimentally. In attempting to increase the theoretical scattering by increasing the factor $FV_0(\delta\rho/\rho)^2$ in Eq. (10), one is faced with the difficulty of constructing a model which provides sufficient scattering, yet is consistent with the known density of the material.

In view of the difficulty in constructing a model to produce strong Rayleigh scattering, it is interesting to note that sufficient scattering can be provided by tunneling states alone. A constant density η_0 of tunneling states, as a function of energy ϵ, is the usual assumption to explain the approximately T^2 behavior of κ and the linear term of the excess specific heat. Acoustic dispersion measurements[13] on fused quartz require an additional quadratic term in the density of states η to explain the data,

$$\eta(\epsilon) = \eta_0 [1 + \gamma(\epsilon/k)^2] , \qquad (11)$$

where the value of γ is ≈ 0.08 K^{-2}. The quadratic term can also explain the "excess" T^3 term in the measured specific heat[20] and, in fact, the coefficient γ deduced from the dispersion measurements is the same as that deduced from the specific-heat

measurements. If the density of tunneling states is accurately described by Eq. (11), then the phonon mean free path l_A [Eqs. (8) and (9)] should be multiplied by $[1 + \gamma(\hbar\omega/k)^2]^{-1}$. From specific-heat measurements on a borosilicate glass,[20] we find a similar coefficient γ to that for fused quartz. If the calculation of κ is now repeated including the factor in Eq. (11), but with no Rayleigh scattering ($B = \infty$), the result gives rather good agreement with the measured data.[51] This agreement is perhaps fortuitous since the tunneling model has been extrapolated beyond the low-temperature region where the parameters were determined.

In summary we have difficulty explaining the magnitude of B in Fig. 5(a) in terms of Rayleigh scattering. This is true for either the Walton or the tunneling model. On the other hand the tunneling model can, using parameters consistent with acoustic and calorimetric measurements, provide the required frequency dependence of the phonon mean free path.

So far we have noted that more than one model may be made to agree with the data on the nonporous glass samples. In comparing theory with data from the porous samples we will use only the models which include Rayleigh scattering. This is primarily a matter of mathematical convenience in representing the strong frequency dependence of $l(\omega)$. Using the parameters thus determined for the scattering in the bulk material, the curves for the porous glass samples have been calculated and included in Fig. 6. The agreement is in all cases good at high and at low temperatures but becomes progressively worse for either model near ≈ 4 K as l_h becomes smaller in magnitude. This might be a failure of the models, or it could be the failure of our assumption that the reflection of phonons from the holes is essentially specular.[23] At lower temperatures the present κ data are consistent with specular reflection. At shorter phonon wavelengths near 10 K ($\lambda \approx 20$ Å) this may not be true, especially since the surfaces had been chemically etched during manufacture, and etching can produce a rough surface.[23,42] A sample was therefore broken and the surfaces of the pores examined in a scanning electron microscope. Indeed the surfaces were rough, but a definitive conclusion could not be obtained. Were only nonspecular scattering present, one may observe from the insert of Fig. 2 that the net mean free path l_h would be reduced by a factor which might be as large as 3 or 4. This would greatly improve the agreement between calculation and data in Fig. 6, but a detailed calculation would require a knowledge of the amount of nonspecular reflection as well as its frequency dependence.

In comparing the models with the polycarbonate data, the results are similar and so only the

tunneling model (with Rayleigh scattering) is shown in Fig. 3. For either model l_B had to be rewritten as $B(\hbar\omega/k)^{-3}$ to fit the data of the nonporous samples. We cannot be certain if the ω^{-3} dependence is indicative of a different scattering process than in the glass,[52] or if the scattering has been complicated by the presence of a slight crystallinity. The curve in Fig. 3 for the nonporous sample has parameters $A = 3.6 \times 10^{-4}$ cm K, $B = 1.6 \times 10^{-3}$ cm K^3, $l_C = 6 \times 10^{-8}$ cm, and $\beta = 1$ K^{-2}. As before, these parameters are used to describe the bulk scattering in the porous samples. For the porous samples the fit is very good with the largest discrepancy occurring for the one curve shown in Fig. 3 which is intended to fit the data of sample $P4$. We believe that all of the data for this sample lie uniformly $\approx 10\%$ low. Even so, the data are depressed near ≈ 2 K suggesting that a frequency-dependent nonspecular reflection of phonons is again occurring at the surfaces of the holes. Because of the low porosity the effect in this case can only be $\approx 30\%$, which is consistent with the data.[53]

V. CONCLUSIONS

The data presented here for two very different materials behave qualitatively in the same manner, and thus the results are probably applicable to most noncrystalline materials. We therefore conclude that thermal transport in noncrystalline materials is predominately by acoustic phonons. In the plateau region of the thermal conductivity, most of the heat flux is carried by low-frequency phonons due to an abrupt decrease in the phonon mean free path with increasing frequency. The temperature range in which the plateau appears is rather insensitive to the characteristics of the amorphous material, again because of the abrupt decrease in mean free path. The measured specific heat, in excess of that contributed by the acoustic phonons, is related to localized or non-propagating excitations.

Certain models of the thermal conductivity of amorphous material, such as that of Klemens, are not compatible with our data. Two models, that of Walton and that of Phillips and of Anderson *et al.*, are both compatible with our measurements. The present data therefore do not by themselves provide a definitive choice between these models, which incorporate very different physical assumptions.

APPENDIX A: PHONON DIFFRACTION

At sufficiently low temperatures in the porous samples the dominant thermal-phonon wavelength λ should become so large that the waves diffract about the holes, and hence the phonon mean free path l_h should increase relative to values at higher temperatures. We would not expect diffraction effects above 0.1 K for the polycarbonate with 2000- or 8000-Å-diam holes, but would expect an increase in l near a few tenths of a Kelvin for that with 300-Å-diam holes. In Fig. 7 we have plotted the ratio of κ for the sample with 300-Å holes, divided by that of the smoothed, averaged κ of the 2000- and 8000-Å data. All three samples have nearly the same l, and hence κ. The ratio of Fig. 7 is constant to within 1% from 0.2 to 1 K, a region in which scattering by holes dominates. But the ratio increases below 0.2 K as diffraction becomes important. It should be noted that other samples had a smaller thermal conductance than the 300-Å sample and thus this increase cannot be attributed to some heat-leak or thermometry problem.

To calculate the diffraction effect we use the same approach outlined in Sec. IV except

$$l_h = l_1 \qquad \text{for } \omega > \omega_1 , \tag{A1}$$

$$l_h = l_1(\omega_1/\omega)^3 \quad \text{for } \omega < \omega_1 , \tag{A2}$$

where l_1 is the value of l_h at short wavelengths (i.e., no diffraction: $0.59d/r$), and ω_1 is the frequency at which diffraction effects begin. We would expect a value for ω_1 such that $qa = (\omega_1/\overline{v}) \times (d/2) = z$, where z is a constant near unity, q is the phonon wave number, and a is the hole radius. A proper theoretical value for z should take account of the various polarizations and propagation
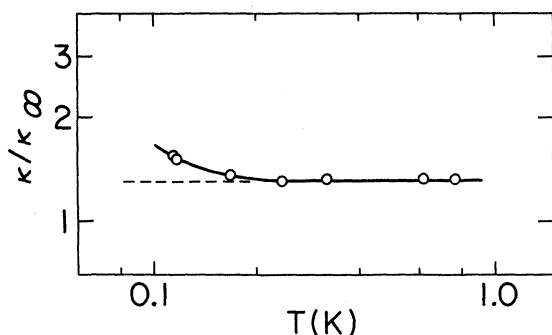

FIG. 7. Thermal conductivity κ of a polycarbonate sample containing $\approx$ 300-Å-diam holes (sample $P6$), divided by the thermal conductivity κ_∞ of samples having much larger hole diameters but nearly the same $l_{h\cdot}$ Increase in the ratio below 0.2 K is due to diffraction of phonons past the 300-Å holes. Estimated uncertainty in this ratio is no more than 2–3%, or less than the size of the points.
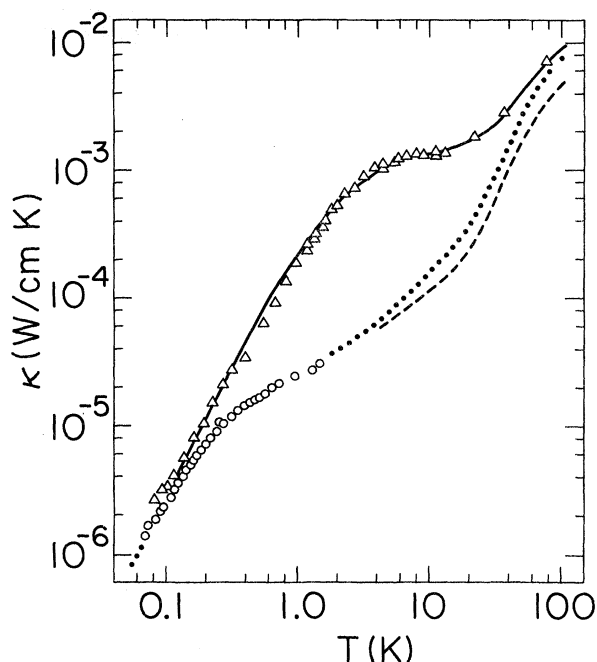

FIG. 8. Thermal conductivity κ of fused quartz ($\triangle$, from Ref. 58) and of two samples of Vycor (o, from Ref. 57) showing the decrease in κ in the Vycor due to the pores. Solid curve is a fit to the fused quartz to obtain the frequency dependence of the phonon mean free path in the bulk material. Dotted lines is a fit to the Vycor using this mean free path plus the additional scattering from the pores. Dashed curve is explained in the text.

directions of the phonons relative to the axes of the holes. This problem, however, is complicated[54,55] and therefore we have used a simplified model (phonons traveling perpendicular to the axes, no distinction between modes) to get a theoretical prediction of $z \approx 0.6$. To fit the curve in Fig. 7 for a hole diameter of $\approx$ 300 Å requires $z \approx 0.3$. This is reasonable agreement considering the uncertainties involved.

A more stringent test is provided by Vycor glass. Vycor is a two-phase glass with one phase having been leached out to leave a silica glass matrix containing a myriad of interconnected holes. This remaining phase of Vycor is very much like vitreous silica, as can be seen from the similarity of their sound velocities.[56] The thermal conductivity of Vycor has been measured by Stephens[57] and is shown in Fig. 8.

We now show that the thermal conductivity of Vycor can be calculated from κ of vitreous silica with the inclusion of phonon scattering from the pores. As a first step the κ of fused silica is computed using, for simplicity, the Walton model. The result is shown in Fig. 8 and compared with the measurements made on fused silica by Zeller.[58]
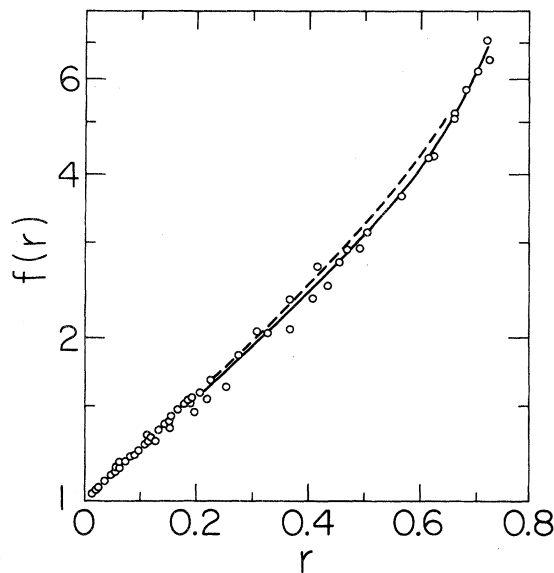
FIG. 9. Plot of the factor f, with which the measured thermal conductance of porous samples must be multiplied to account for the missing material, as a function of the porosity r. Points were measured in an electrical analog as discussed in the text; solid curve is a fit to these data. Dashed curve is the result of a simplified calculation.

The parameters A, B, etc., in this calculation are now considered to be constants.

Next, using Eqs. (A1) and (A2), the excellent fit shown by the dotted line in Fig. 8 is obtained for Vycor with $l_1\omega_1^3 = 2.1\times10^{-3}(k/\hbar)^3$ cm K^3. Any value of l_1 in Eq. (A1), so long as $l_1 \lesssim 500$ Å, does not alter κ in the low-temperature region where the experimental data exist. Since for Vycor we expect l_1 (= 0.59d/r) to be less than 500 Å, we cannot deduce a value for l_1 from these data. Using the value found for $l_1\omega_1^3$ as well as the volume porosity ($\approx 33\%$) and hole diameter (≈ 60 Å) determined by gas adsorption measurements,[59,60] we obtain $z \approx 1.2$. This is somewhat larger than the value of z determined from the polycarbonate data, but may not be unreasonable in light of the very different shapes of the pores in the two materials. In fact, one would expect the very contorted pores in Vycor to produce more diffraction at a given wavelength, and this corresponds to a larger value of z.

The Vycor data of Fig. 8 have not been corrected for the "missing volume" of the pores since in the long-wavelength limit, where diffraction dominates, the entire cross section of the *sample* partakes in thermal transport. However for the higher-frequency phonons the factor of Appendix B becomes significant. The dashed curve in Fig. 8 indicates the expected magnitude of the raw data; correction for the missing volume would move the data up to the dotted curve. Below 4 K the difference is negligible.

The measurements on polycarbonate and on Vycor discussed in this appendix demonstrate the diffraction of thermal phonons about pores when $\lambda > d$. The agreement between the data and our calculations lends further support to the picture of phonon behavior depicted in Fig. 5.

APPENDIX B: MISSING-VOLUME FACTOR

If holes are introduced in a solid sample of fixed size, the thermal conductance is decreased because there is a smaller volume for the heat to flow through. The problem of determining this change in conductance can be solved mathematically,[61] but if the holes are randomly placed the calculation becomes rather complicated. Since our samples are essentially two-dimensional (the cylindrical holes are perpendicular to the plane of the samples), the problem can be solved empirically. The geometry was simulated electrically using electrically conducting paper with appropriate holes cut out, and with silver paint to provide the equipotentials representing isotherms.

First, the resistance of the paper was measured, then four separate measurements were made with different hole patterns cut in the paper. These were (i) uniform holes randomly placed, (ii) uniform holes placed in a honeycomb pattern, (iii) a single hole in the center of a square which, by symmetry, is equivalent to many holes placed on a square-grid pattern, and (iv) two quarter-circles cut from opposite corners of a rectangle which is equivalent to the honeycomb pattern. The results are shown in Fig. 9 as the function $f(r)$= (resistance with holes)/(resistance without holes). All four hole patterns gave the same results. A mathematical approximation[63] gave the broken line in Fig. 9 which agrees very well with the measurements. In applying this factor to our data, the experimental result represented by the solid line was used.

[1]C. Kittel, Phys. Rev. 75, 972 (1949).
[2]P. G. Klemens, Proc. R. Soc. A 208, 108 (1951).
[3]A. C. Anderson and R. B. Rauch, J. Appl. Phys. 41, 3648 (1970).
[4]R. C. Zeller and R. O. Pohl, Phys. Rev. B 4, 2029 (1971).

[5]A. J. Leadbetter, in *Proceedings of the International Conference on Phonon Scattering in Solids*, edited by H. J. Albany (La Documentation Francaise, Paris, 1972), p. 338, and papers cited therein.

[6]H. Böttger, Phys. Status Solidi B __62__, 9 (1974), and papers cited therein.

[7]G. K. Chang and R. E. Jones, Phys. Rev. __126__, 2055 (1962).

[8]P. Fulde and H. Wagner, Phys. Rev. Lett. __27__, 1280 (1971).

[9]K. S. Dubey, Solid State Commun. __15__, 875 (1974), and papers cited therein.

[10]G. J. Morgan and D. Smith, J. Phys. C __7__, 649 (1974).

[11]D. Walton, Solid State Commun. __14__, 335 (1974).

[12]W. Arnold, S. Hunklinger, S. Stein, and K. Dransfeld, J. Non-Cryst. Solids __14__, 192 (1974), and papers cited therein.

[13]L. Piche, R. Maynard, S. Hunklinger, and J. Jäckle, Phys. Rev. Lett. __32__, 1426 (1974).

[14]G. K. White, Phys. Rev. Lett. __34__, 204 (1975).

[15]A. S. Pine, Phys. Rev. __185__, 1187 (1969).

[16]Y. Y. Huang, J. L. Hunt, and J. R. Stevens, J. Appl. Phys. __44__, 3589 (1973).

[17]W. F. Love, Phys. Rev. Lett. __31__, 822 (1973), and papers cited therein.

[18]H. Happel, K. Knorr, and N. Barth, Z. Phys. __249__, 185 (1971), and papers cited therein.

[19]F. R. Ladan and A. Zylbersztejn, Phys. Rev. Lett. __28__, 1198 (1972).

[20]R. B. Stephens, Phys. Rev. B __8__, 2896 (1973), and papers cited therein.

[21]J. Szeftel and H. Alloul, Phys. Rev. Lett. __34__, 657 (1975), and papers cited therein; P. C. Taylor and M. Rubinstein, in *Amorphous and Liquid Semiconductors*, edited by J. Stuke and W. Brenig (Taylor and Frances, London, 1974), p. 1161.

[22]A preliminary report of this work has been published; M. P. Zaitlin and A. C. Anderson, Phys. Rev. Lett. __33__, 1158 (1974).

[23]M. P. Zaitlin, L. M. Scherr, and A. C. Anderson, Phys. Rev. B __12__, 4487 (1975).

[24]Galileo Electro-Optics, Inc., Galileo Park, Sturbridge, Mass. 01518. The glass from which the array is constructed is Kimble EN1.

[25]Nuclepore Corp., 7035 Commerce Circle, Pleasanton, Ca. 94566. This material is irradiated and chemically etched to produce holes. The original material was supplied by Peter J. Schweitzer, Division of Kimberly-Clark, Lee, Mass. 01238.

[26]J. M. Ziman, *Electrons and Phonons* (Oxford U. P., London, 1963).

[27]G. J. Sellers and A. C. Anderson, Rev. Sci. Instrum. __45__, 1256 (1974).

[28]A. C. Anderson, R. E. Peterson, and J. E. Robichaux, Rev. Sci. Instrum. __41__, 528 (1970).

[29]W. L. Johnson and A. C. Anderson, Rev. Sci. Instrum. __42__, 1296 (1971).

[30]R. Berman, Phys. Rev. __76__, 315 (1949); see also R. W. B. Stephens, Philos. Mag. __14__, 897 (1932).

[31]A. C. Anderson, W. Reese, and J. C. Wheatley, Rev. Sci. Instrum. __34__, 1386 (1963).

[32]R. A. Fisher, G. E. Brodale, E. W. Hornung, and W. F. Giauque, Rev. Sci. Instrum. __39__, 108 (1968).

[33]R. E. Peterson and A. C. Anderson, Rev. Sci. Instrum. __43__, 834 (1972).

[34]R. B. Stephens, G. S. Cieloszyk, and G. L. Salinger,

Phys. Lett. A __38__, 215 (1972).

[35]G. S. Cieloszyk, M. T. Cruz, and G. L. Salinger, Cryogenics __13__, 718 (1973). We estimate the Debye frequency to be $\hbar\omega_D/k = 120$ K; see Ref. 62.

[36]W. Reese, J. Macromol. Sci. Chem. A __3__, 1297 (1969).

[37]G. L. Salinger, in *Amorphous Materials*, edited by R. W. Douglas and B. Ellis (Wiley-Interscience, New York, 1970), p. 475.

[38]K. W. Garrett and H. M. Rosenberg, in Proceedings of the ICEC4, Eindhoven, 1972, p. 267 (unpublished).

[39]C. Schmidt, Cryogenics __15__, 17 (1975).

[40]Here $\bar{v} = v_t [\frac{1}{3}(2 + v_t^2/v_l^2)]^{-1/2}$, where v_t and v_l are the transverse and longitudinal sound velocities.

[41]At 10^7 Hz we obtain for the glass $v_t = 3.19 \times 10^5$ cm/sec at 300 K and $v_t = 3.17 \times 10^5$ cm/sec at 77 K. At 300 K we obtain $v_l = 5.17 \times 10^5$ cm/sec. We estimate the Debye frequency to be $\hbar\omega_p/k = 300$K; see Ref. 62.

[42]R. O. Pohl, W. F. Love, and R. B. Stephens, in *Amorphous and Liquid Semiconductors*, edited by J. Stuke and W. Brenig (Taylor and Francis, London, 1974), p. 1121.

[43]For example, see P. North and K. L. Chopra, Phys. Rev. B __10__, 3412 (1974).

[44]P. G. Klemens, Proc. R. Soc. A __208__, 108 (1951).

[45]P. G. Klemens, in *Physics of Non-Crystalline Solids*, edited by J. A. Prins (North-Holland, Amsterdam, 1965), p. 162.

[46]B. Dreyfus, N. C. Fernandes, and A. Maynard, Phys. Lett. A __26__, 647 (1968). The frequency dependence of phonon scattering at low frequencies is not correct in this paper.

[47]L. A. Chernov, *Wave Propagation in a Random Medium* (McGraw-Hill, New York, 1960).

[48]W. A. Phillips, J. Low Temp. Phys. __7__, 351 (1972).

[49]P. W. Anderson, B. I. Halperin, and C. M. Varma, Philos. Mag. __25__, 1 (1972).

[50]J. Jäckle, Z. Phys. __257__, 212 (1972). In terms of parameters used by Jäckle, $\beta = 7.21(v_l^{-5} + 2v_t^{-5})B^2k^2/\pi^2\rho\hbar^3$ and $A = \rho v^3\hbar/\pi B^2 Pk$.

[51]This is discussed in more detail by M. P. Zaitlin and A. C. Anderson, Phys. Status Solidi B __71__ (to be published).

[52]The ω^{-3} dependence would be indicative of scattering from a one-dimensional object in the shape of a long rod of diameter small compared to the phonon wavelength. Alternatively, agreement could be obtained using only tunneling states, without "Rayleigh" scattering, as for the glass samples.

[53]For small porosity and entirely nonspecular reflection from the surfaces of the holes (which produces a different angular distribution of scattered phonons than in the specular case), $l = 0.56/nd = 0.44 d/r$.

[54]P. M. Morse and K. V. Ingard, *Theoretical Acoustics* (McGraw-Hill, New York, 1968), pp. 401–405.

[55]A. S. Bolubev, Akust. Zh. __7__, 174 (1961) [Sov. Phys.-Acoust. __7__, 138 (1961)]; R. M. White, J. Acoust. Soc. Am. __30__, 771 (1958).

[56]The room-temperature sound velocities in Vycor as calculated from the elastic constants provided to us by Corning Glass Works, Corning, N. Y., are within a few precent of the sound velocities of fused quartz as determined by Love, Ref. 17.

[57]R. B. Stephens, Ph. D. thesis (Cornell University, 1974) (unpublished).

[58]R. C. Zeller, M. S. thesis (Cornell University, 1971) (unpublished), including corrections by Stephens, Ref.

57. For the calculation, $\hbar\omega_p/k = 343$ K (Ref. 62), $\bar{v}$ $= 4.12 \times 10^5$ cm/sec (Ref. 17), $A = 4.3 \times 10^{-3}$ cm K, B $= 0.97$ cm K^4, $l_C = 1.0 \times 10^{-7}$ cm.

[59] D. F. Brewer and D. C. Champeney, Proc. Phys. Soc. Lond. 79, 855 (1962).

[60] Values quoted for the pore diameter range from 45 to 75 Å, with a volume porosity of $\approx 33\%$. We thank T. Elmer of Corning Glass Works for a discussion concerning Vycor.

[61] H. W. Russel, J. Am. Ceram. Soc. 18, 1 (1935); W. Woodside, Can. J. Phys. 36, 815 (1958); D. J. Jeffrey, Proc. R. Soc. A 335, 355 (1973); R. E. Meredith and C. W. Fobias, J. Appl. Phys. 31, 1270 (1960).

[62] O. L. Anderson, J. Phys. Chem. Solids 12, 41 (1959).

[63] M. P. Zaitlin, Ph. D. thesis (University of Illinois, 1975) (unpublished).